Australian Journal of Basic and Applied Sciences

ISSN :1991-8178
EISSN: 2309-8414

2022 April; 16(4): pages 1-10
https://doi.org/10.22587/ajbas.2022.16.4.1

Research Paper AENSI Publications

Eucalyptol inhaled during Invasive Mechanical Ventilation may attenuate Lung Injury caused by oxygen therapy in the management of COVID-19

Daniel Silveira Serra[1*], Leidianne Costa da Silva Andrade[2], Marcelle Ferreira Moura[2], Soujanya Talapala Naidu[2], Allison Matias de Sousa[2], Fladimir de Lima Gondim[2], Francisco Sales Ávila Cavalcante[1].

[1] State University of Ceará, Sciences and Technology Center, physics faculty, Fortaleza-Brazil, Brazil
[2] State University of Ceará, Institute of Biomedical Sciences, Faculty of physiology, Fortaleza-Brazil, Brazil

Correspondence Author: Daniel Silveira Serra1, State University of Ceará, Sciences and Technology Center, physics faculty, Fortaleza-Brazil, Brazil
daniel.silveira@uece.br

Received date: 12 February 2022, Accepted date: 22 March 2022, Online date: 15 April 2022

Citation: D. S. Serra., L. C.da S. Andrade., M. F. Moura., S. T. Naidu., A. M. de Sousa., F. de Lima. Gondim., F. S. Á. Cavalcante. (2022). Eucalyptol inhaled during Invasive Mechanical Ventilation may attenuate Lung Injury caused by oxygen therapy in the management of COVID-19. Australian Journal of Basic and Applied Sciences, 16(4): 1-10. DOI: 10.22587/ajbas.2022.16.4.1.

ABSTRACT: INTRODUCTION: Patients who develop Severe Acute Respiratory Syndrome caused by Coronavirus-2 (SARS-CoV-2) may be admitted to an Intensive Care Unit (ICU) and be subjected to prolonged Invasive Mechanical Ventilation (IMV) to receive adequate oxygen therapy. However, IMV associated with high concentrations of oxygen may lead to Hyperoxic Acute Lung Injury (HALI) and Ventilator-Induced Lung Injury (VILI). In an attempt to minimize the risk of pulmonary damage, the following hypothesis was raised: Would the association of Eucalyptol inhalation to IMV with a high FiO2 be a suitable measure to decrease the secondary lung injury caused by VILI and HALI during SARS-CoV-2 Disease (COVID-19) treatment? METHODS: In order to answer this question, the use of nebulized Eucalyptol during IMV with 100% FiO2 was investigated, by analyzing respiratory mechanics in vivo and lung histopathology and parenchymal morphometry in vitro. 24 animals were randomly divided into 3 groups: one subjected to 30 minutes of IMV with 21% FiO2 plus nebulized saline (Group 21%+S), one group subjected to 30 minutes of IMV with 100% FiO2 plus nebulized saline (Group 100%+S), and a third group subjected to 30 minutes of IMV plus 100% FiO2 and nebulization with 10 mg/mL Eucalyptol (Group 100%+E). RESULTS: Changes were demonstrated in all respiratory mechanics parameters for the animals in the 100%+S group, as compared with those in the 21%+S group, indicating the presence of secondary lung injury associated with VILI and/or HALI. A statistically significant decrease was also observed for the respiratory mechanics variables of the animals in the 100%+E group when compared with data from the 100%+S group, indicating attenuation of the secondary pulmonary damage due to VILI and/or HALI. CONCLUSION: Treatment with nebulized Eucalyptol at a dose of 10 mg/mL attenuates pulmonary lesions due to HALI and VILI, thus presenting as an attractive option for COVID-19 management in patients under IMV with high values of FiO2.

Keywords: SARS-CoV-2, COVID-19, VILI, HALI, Eucalyptol

INTRODUCTION

Patients with preexisting ailments, such as hypertension, cardiovascular disease, diabetes, chronic respiratory illnesses, or cancer, are at a greater risk of developing Severe Acute Respiratory Syndrome caused by Coronavirus-2 (SARS-CoV-2) (Zhou et al., 2020). Moreover, the severity of SARS-CoV-2 Disease (COVID-19) is closely related to its prognosis. Therefore, basic and essential strategies must be implemented to rapidly detect high-risk patients to afford adequate early treatment. While most hospitalized patients need only non-invasive oxygen therapy (including non-invasive ventilation [NIV]) as the optimal treatment, many patients with COVID-19 develop severe respiratory distress, hypoxemia, or hemodynamic instability. Such patients require

admission to an Intensive Care Unit (ICU) and, in some cases, use of prolonged invasive mechanical ventilation (IMV) (Sun et al., 2020; Richardson et al., 2020) to receive adequate oxygen therapy to maintain a blood oxygen saturation ($SatO_2$) > 94% (WHO 2020; Rello et al., 2020). IMV allows patients to receive a fraction of inspired oxygen (FiO_2) of up to 100%. However, prolonged administration of high oxygen concentrations can lead to toxic effects that may result in Hyperoxic Acute Lung Injury (HALI), thus aggravating pulmonary inflammation and causing apoptotic epithelial cell death (Li, 2007). Moreover, IMV in high-risk patients has been seen to increase pulmonary injury caused by severe acute respiratory syndrome (SARS), leading to ventilator-induced lung injury (VILI) (Nieman et al., 2017). Thus, IMV may induce VILI and lead to a worsened prognosis for COVID-19 patients. Therefore, it is necessary to seek treatment strategies that prevent IMV-associated pulmonary injury, which could save the lives of a large number of patients (Barrasa et al., 2020).

In addition, there is a significant contribution of angiotensin-converting enzyme (ACE) to the interaction between SARS-CoV-2 and human cells. This interaction causes an increase in angiotensin II (Zou et al., 2020), a peptide involved in inflammation, decreased alveolar fluid clearance, and remodeling in lung tissue (Ismael-Badarneh et al., 2015; Forrester et al., 2018). For this reason, studies involving compounds capable of promoting ACE inhibition and the suppression of cytokines produced from viral infection are necessary (Sriram; Insel., 2020; Chen et al., 2020).

One possible means to reduce pulmonary damage resulting from HALI and/or VILI (a potential side effect during the management of severe COVID-19) would be to employ a natural product such as Eucalyptol in association with IMV. Eucalyptol (also known as 1,8-Cineol) is a major constituent of the oil obtained from the leaves of eucalyptus species, such as *Eucalyptus globulus* Labill. It is a terpenoid with anti-inflammatory properties free of the side effects commonly observed during corticosteroids.

Studies have shown that Eucalyptol possesses biological activity that includes various mechanisms and several notable molecules capable of curtailing the development of inflammation in the respiratory system, such as reduction of tracheobronchial resistance (Nascimento et al., 2009), downregulation of molecules involved in mucus production, and promotion of anti-inflammatory activity in asthmatic subjects (Zhou et al., 2007). In addition, Eucalyptol had the potential to inhibit ACE, and reduce the expression of NF-κB, proteases and several pro-inflammatory cytokines (Dey et al., 2014; Kim et al., 2015).

With the above findings in mind, the following hypothesis was raised: Could Eucalyptol inhalation be used as a strategy to reduce secondary pulmonary damage caused by VILI and HALI arising from high-FiO_2 IMV during the management of severe COVID-19? To answer this question, this work aimed to investigate the use of nebulized Eucalyptol during IMV with a high FiO2 by analyzing respiratory mechanics in vivo and pulmonary histopathology parenchymal morphometry *in vitro*.

MATERIALS AND METHODS

2.1 Animals

Male Wistar rats (7-8 weeks of age), with an average body mass of 200 ± 50 g were fed with chow and to water *ad libitum*, and housed in a controlled environment (18–22 °C, 50–70% relative humidity, 12/12 h light/dark cycle), were used in this study. The rats were housed in plastic cages under controlled environmental conditions. The animal ethics committee of the Ceará State University (CEUA-UECE) had previously approved all animal use and care procedures.

24 animals randomly divided into three groups (n = 8) were used. To simulate IMV without supplemental oxygen and no combined treatment, the first group was subjected to 30 minutes of IMV with a FiO_2 of 21% and nebulized saline (Group 21%+S). Next, a simulation of IMV associated with a high oxygen fraction was performed utilizing a second group subjected to 30 minutes of IMV with a FiO_2 of 100% and nebulized saline (Group S+100%). Finally, a simulation of IMV with high-concentration oxygen therapy and an associated treatment was performed using a third group subjected to 30 minutes of IMV with an FiO_2 of 100% and nebulization with 10 mg/mL of Eucalyptol (Sigma Chemical Co., St. Louis, MO, USA) (Group 100%+E). This dosage was chosen based on a previous study that used nebulized Eucalyptol to treat acute lung inflammation (Kennedy-Feitosa et al., 2016).

2.2 Experimental protocol

All respiratory system mechanics data were collected through an experimental platform (Figure 1). The platform contained a mechanical ventilator for small animals (Figure 1A), a receptacle for the nebulization solution (Figure 1B), and an ultrasonic nebulizer (Figure 1C) attached to a water bath (Figure 1D), which maintained the solution at 37°C. Cylinders of compressed air (Figure 1E) and oxygen (Figure 1F) were attached to a blender (Figure 1G), where the required FiO_2 (21% or 100%) was adjusted and later directed to the ventilator. The test subjects were connected to the mechanical ventilator using a tracheal cannula (Figure 1H).

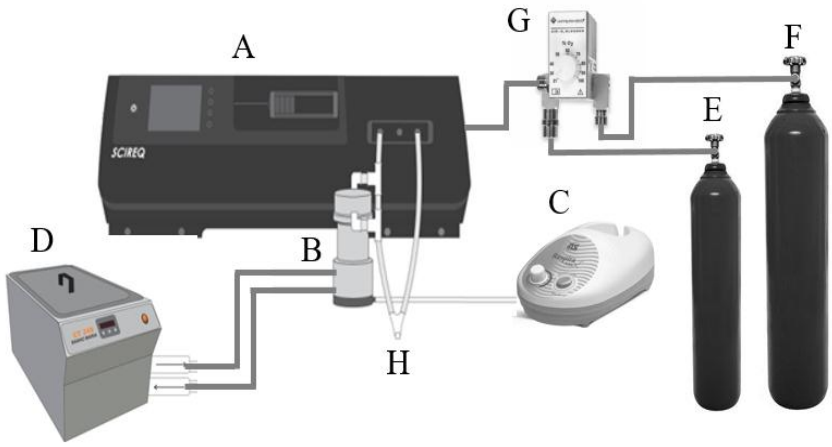

Figure 1. Experimental Platform. A- Mechanical ventilator for small animals; B- Receptacle for the inhaled solution; C- Ultrasonic nebulizer; D- Heating bath; E- Compressed air cylinder; F- O_2 cylinder; G- Blender; H- Cannula for subjection connected to the ventilator.

2.3 Respiratory system mechanics

Animals were anaesthetized (ketamine: xylazine 100:10 mg/kg), tracheostomized, intubated (using a 14-gauge cannula) and then connected to a computer-controlled ventilator for small animals (Scireq© - *flexiVent*®, Montreal, QC, Canada). Subjects were then submitted to neuromuscular blockade (pancuronium bromide - 0.5 mL/kg, ip, Cristália, Brazil) and ventilated at baseline patterns at a frequency of 90 breaths/min, tidal volume of 10 mL/kg, with a pressure limit of 30 cm·H_2O, and positive end-expiratory pressure (PEEP) of 3 cm·H_2O.

Immediately after standardization of the mechanical history, respiratory system impedance (Z_{rs}) was measured by the forced oscillation technique (FOT) (Hantos et al., 1992), using 12 sequential 30 s-sampling intervals for a total of 6 minutes (12 total). The FOT allows the acquisition of information regarding Newtonian resistance (R_N), tissue elastance (H), and tissue resistance (G). Following this procedure, five quasi-static PV curves were obtained to measure C_{ST}, an estimate of inspiratory capacity (IC), and PV loop area. Measurements of the respiratory system mechanics mentioned above were performed at two different times. The first measurement occurred immediately after the animals were connected to the ventilator (Subgroups 21%+S-0', 100%+S-0' and 100%+E-0'). The second set was performed after 30 minutes of ventilation using the respective nebulization solution for each group. Respiratory system mechanics data were analyzed in terms of Newtonian resistance variation (ΔR_N), elastance variation (ΔH) and tissue resistance change (ΔG), for those measurements pertaining to the constant phase model. Variations of compliance (ΔC_{ST}), inspiratory capacity (ΔCI) and in PV loop area ($\Delta Area$) were also analyzed for those measurements referring to the PV curve. It was adopted Δ as the parameter at time 30' minus its value at time 0'; for these calculations, all values were standardized according to the 0' time values. Thus, results pertaining to respiratory system mechanics will be presented as a function of increased or decreased fractions of the respective variables after 30 minutes of IMV.

2.4 Histological study

After determination of the respiratory system mechanics, left lung was kept at functional residual capacity and fixed in Millonig's formaldehyde (100 mL HCHO, 900 mL H_2O, 18.6 g NaH_2PO_4, 4.2 g NaOH). Glass slides containing sections of the lung were stained with hematoxylin and eosin (HE) and examined by optical microscopy according to their qualitative and quantitative aspects.

The point-counting technique determined the fraction area of alveolar collapse and the amount of polymorphonuclear (PMN) cells and pulmonary tissue (Weibel et al., 1990). Air-space enlargement was quantified by the mean linear intercept length of the distal air spaces (L_m) in 30 randomly chosen fields of tissue sections per group (Knudsen et al., 2010). Cellularity was assessed at 1000x magnification across 10-15 random non-coincident microscopic fields in each animal. Morphometric analyses and determination of bronchoconstriction indices were performed at 400x magnification. Bronchoconstriction index (BCI) was determined in 10 non-coincident microscopic fields per animal, using a reticulum and applying the equation 1 (Sakae et al., 1994):

$$BCI = \frac{NI}{\sqrt{NP}} \quad (1)$$

where NP is number of points in the airway lumen and NI is intercepts through the airway wall.

2.5 Statistical Analyses

Statistical analyses were performed using GraphPad Prism version 5.00 (GraphPad, San Diego, CA, USA). Results are presented as mean ± SD, where *n* represents the number of samples. We used a one-way analysis of variance (ANOVA) to compare groups, followed by the Student–Newman–Keuls test. Multiple comparisons were then corrected with a Bonferroni test. A difference was considered significant if $p < 0.05$.

RESULTS

Figure 2 shows the respiratory system analyses for animals of the three groups: Group 21%+S (ΔR_N= 0.078±0.025, ΔG= 0.091±0.043, ΔH= 0.117± 0.052, ΔC_{ST}= -0.097±0.048, ΔCI= -0.062±0.026, $\Delta Area$= 0.085±0.031) underwent IMV with 21% FiO_2 and 30 minutes of saline nebulization; Group S+100% (ΔR_N= 0.754±0.182, ΔG= 0.836±0.250, ΔH= 0.912±0.351, ΔC_{ST}= -.400±0.142, ΔCI= 0.433±0.091, $\Delta Area$ =0.508±0.171) was subjected to IMV with a FiO_2 of 100% plus 30 min of saline nebulization; and Group 100%+E (ΔR_N= 0.268±0.066, ΔG= 0.369±0.129, ΔH= 0.246±0.088, ΔC_{ST}= -0.195±0.074, ΔCI= -0.159±0.074, $\Delta Area$= 0.182±0.075) underwent IMV at 100% FiO_2 and 30 minutes' nebulization with a solution of 10 mg/mL Eucalyptol.

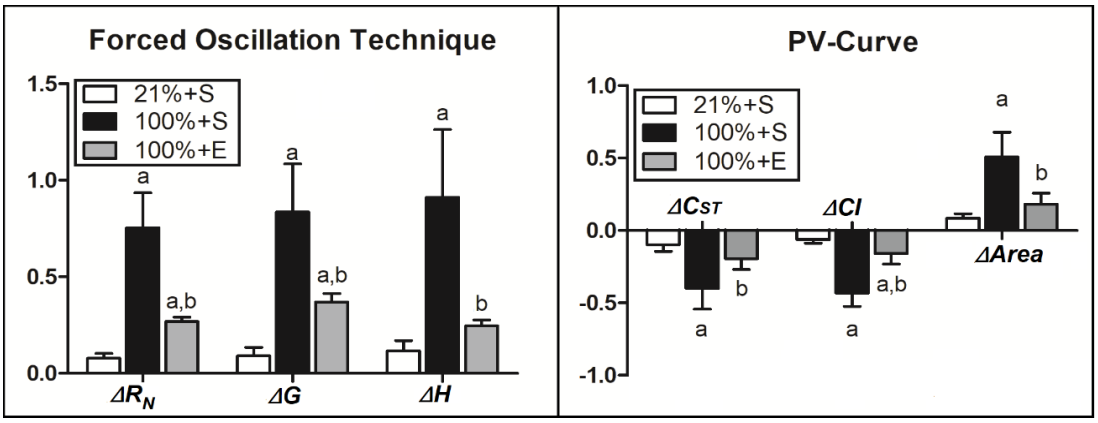

Figure 2. Respiratory system parameters for rats submitted to invasive mechanical ventilation (IMV) with FiO_2 21% and 30 minutes' nebulization with saline (Group 21%+S), or with FiO_2 100% and 30 minutes' nebulization with saline (Group 100%+S) or 10 mg/mL of Eucalyptol (Group 100%+E). Data are presented as a function of the measurements obtained using the Constant Phase Model (ΔR_N: variation in Newtonian resistance, ΔH: variation in tissue elastance, and ΔG: variation in tissue resistance) and PV curve (ΔC_{ST}: variation of static compliance, ΔCI: variation in inspiratory capacity, and $\Delta Area$: variation of PV Loop area). [a] Different from 21%+S group ($p<0.05$). [b] Different from 100%+S group ($p<0.05$). By one-way ANOVA followed by multiple comparisons corrected with Bonferroni's test.

Figure 3 shows the PV curve graphs. Figure 3A presents the PV curve graphs for Group 21%+S with data from time 0 (21%+S-0') and after 30 minutes of IMV with 21% FiO_2 and saline nebulization (21%+S-30'). Figure 3B shows graphs for Group 100%+S with data from time 0 (100%+S-0') and after 30 minutes of IMV with 100% FiO_2 plus saline nebulization (100%+S-30'). Figure 3C shows graphs for Group 100%+E, with data from time 0 (100%+E-0') and after 30 minutes of IMV with 100% FiO_2 plus nebulization of 10 mg/mL of Eucalyptol (100%+E-30'), as well as for Group 100%+S, with data collected after 30 minutes of IMV and 100% FiO_2 plus saline nebulization (100%+S-30'). PV loops were generated using the data provided by the stepwise PVr-P maneuver.

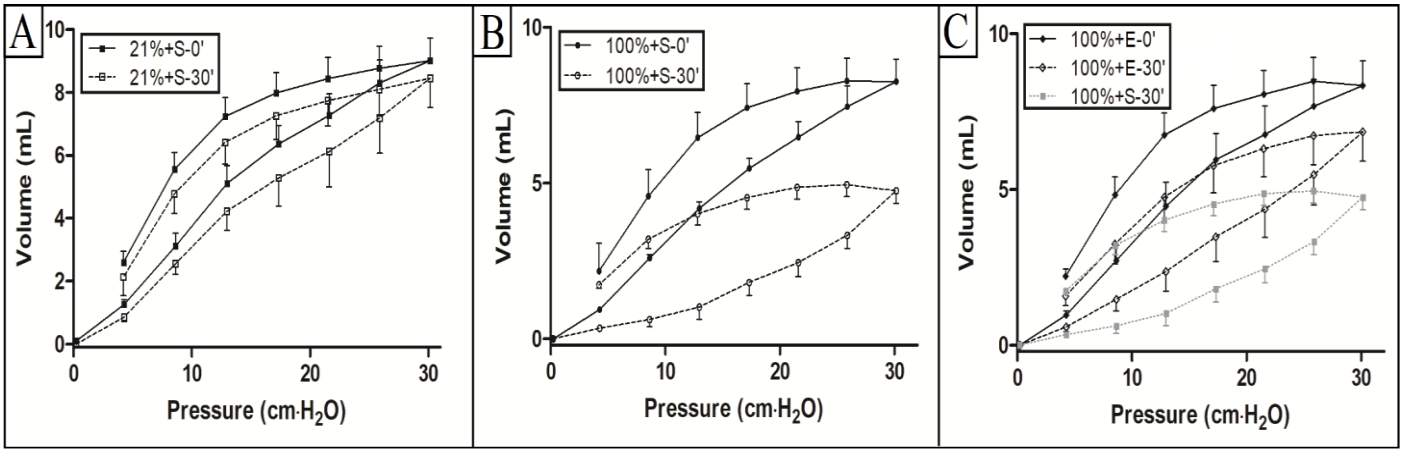

Figure 3. PV curves. A- PV curves for group 21%+S, data collected at time 0 (21%+S-0') and after 30 minutes of ventilation with FiO_2 21% and saline nebulization (21%+S-30'). B- PV curves for group 100%+S, data collected at time 0 (100%+S-0') and after 30 minutes of ventilation with FiO_2 100% and saline nebulization (100%+S-30'). C- PV curves for group 100%+E, data collected at time 0 (100%+E-0') and after 30 minutes of ventilation with FiO_2 100% and nebulization with 10 mg/mL Eucalyptol (100%+E-30'), and for group 100%+S, data collected after 30 minutes of ventilation with FiO_2 100% and saline nebulization (100%+S-30').

Figure 4 depicts representative lung histological images for the 21%+S, 100%+S and 100%+E groups. Alveolar collapse, thickened septa and cellular infiltrates observed in the photomicrographs of the pulmonary parenchyma of the 100%+S and 100%+E groups.

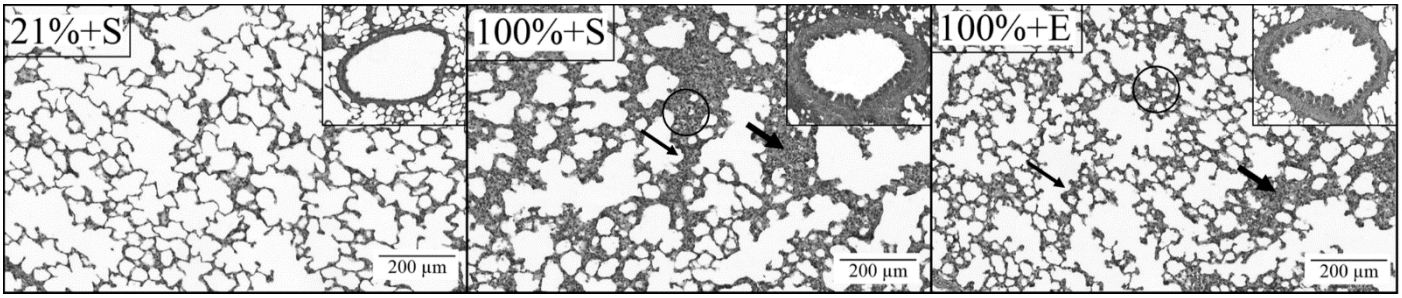

Figure 4. Photomicrographs of lung parenchyma and airway (inserts), stained with hematoxylin-eosin for groups 21%+S, 100%+S and 100%+E. Thin arrows: thickened septa; thick arrows: cellular infiltrates; and circles:

Finally, Table 1 displays alveolar collapse, the quantity of polymorphonuclear cells, mean alveolar diameter, and bronchoconstriction index (BCI) for the three groups. An increase in alveolar collapse, PMN cells, L_m and BCI within the 100%+S group, when compared with the 21%+S group, was observed. Altogether, these findings may suggest pulmonary inflammation and bronchoconstriction caused by invasive mechanical ventilation with 100% FiO_2 for 30 minutes. Furthermore, a statistically significant decrease was also observed in the values of collapsed alveoli and the PMN cells in the 100%+E group compared with the 100%+S group, which demonstrates attenuation in the pulmonary injury caused by invasive mechanical ventilation with 100% FiO_2 during 30 minutes, due to nebulization with Eucalyptol.

Table 1. Morphometric parameters for rats submitted to invasive mechanical ventilation

Groups	Alveolar Collapse (%)	PMN Cells ($x10^{-3}/\mu m^2$)	Mean alveolar diameter (µm)	BCI
21%+S	9.82 ± 1.72	19.44 ± 3.39	40.22 ± 2.77	2.29 ± 0.15
100%+S	23.74 ± 2.74[a]	29.61 ± 4.25[a]	33.39 ± 4.41[a]	2.74 ± 0.20[a]
100%+E	16.12 ± 3.19[a,b]	23.19 ± 3.79[b]	37.51 ± 4.13	2.47 ± 0.28

Morphometric parameters for rats submitted to invasive mechanical ventilation (IMV) with FiO_2 21% and 30 minutes' nebulization with saline (Group 21%+S), or with FiO_2 100% and 30 minutes' nebulization with saline (Group 100%+S) or 10 mg/mL of Eucalyptol (Group 100%+E). Values are mean ± SD of 21%+S, 100%+S and 100%+E groups. Data collection was performed in ten matched fields per rat. PMN, polymorphonuclear cells; BCI, bronchoconstriction index. [a]Different from 21%+S group ($p<0.05$). [b]Different from 100%+S group ($p<0.05$). By one-way ANOVA followed by multiple comparisons corrected with Bonferroni's test.

DISCUSSION

Unfortunately, no vaccines or antiviral drugs currently exist to effectively prevent or treat infection caused by SARS-CoV-2. However, there are significant efforts worldwide to find appropriate therapies. Of note are studies using medications such as chloroquine, hydroxychloroquine, or remdesivir *in vitro* (Yao et al., 2020; Liu et al., 2020; Choy et al., 2020) or *in vivo* (Singh et al., 2020; Chorin et al., 2020), as well as trials using convalescent plasma (Duan et al., 2020; Zhang et al., 2020; Shen et al., 2020). It is estimated that more than 150 drugs are currently being tested for the treatment of COVID-19. In the absence of treatment that could effectively eliminate SARS-CoV-2 from the human body, alternative methods are being evaluated as management strategies suitable for severe and critical patients in medical care facilities. These include invasive mechanical ventilation (IMV) associated with oxygen therapy (Namendys-silva, 2020; Murthy et al., 2020; Taisheng et al., 2020; Wang et al., 2020) in intensive care units (ICU). Approximately 30-40% of patients admitted to the ICU require invasive ventilatory support (ICNARC, 2016). Invasive mechanical ventilation (IMV) occurs when a mechanical ventilator is connected to the patient via an endotracheal or tracheostomy tube, through which it intermittently inflates the airways with volumes of air (tidal volume), which can be predefined. IMV can help stabilize patients with hypoxemic respiratory failure (Kapitan, 2013), decrease inspiratory work of breathing (Reid, 1994), and allow for the implementation of lung-protective (low tidal volume) ventilation in patients with SARS (Brower et al., 2000).

A study that examined adult patients infected with SARS-CoV-2 in the University Hospital of Araba (Vitoria, Spain) suggests that oxygen therapy saves lives. The authors report that even after 15 days of stay in the ICU, half of the study patients were still intubated, while one-third did not survive (Barrasa et al., 2020). Another study that analyzed the use of remdesivir in the treatment of 237 patients admitted to hospital with severe forms of COVID-19 reported that the duration of oxygen therapy for these patients was up to 38 days (an average of 25 days), and that mechanical ventilation lasted for up to 21 days (mean 15.5 days)

(Wang et al., 2020). These studies demonstrate the need for prolonged IMV associated with oxygen therapy for the management of severe cases of COVID-19. However, such therapies can cause Ventilator Induced Lung Injury (VILI) and/or Hyperoxic Acute Lung Injury (HALI). Therefore, there is an urgent need for studies that find treatment strategies to mitigate these secondary lung injuries that may arise and thus worsen the prognoses of critically-ill patients affected by SARS-CoV-2. Based on this—and although in the present study, groups of animals exposed to SARS-CoV-2 were not used, an indirect analysis of the effects of IMV and high-concentration oxygen therapy on the respiratory systems of healthy animals was performed in an attempt to increase knowledge about the mechanical and physiological pulmonary mechanisms involved in VILI and/or HALI. In addition, nebulized Eucalyptol was used as a treatment strategy to mitigate secondary pulmonary lesions caused by VILI and/or HALI.

Regarding the results, respiratory system mechanics were evaluated using the FOT and PV curves (Figure 2). In the FOT, Newtonian resistance (R_N) characterizes an estimate of the total central airway resistance (Bates, 2009); tissue resistance (G) and tissue elastance (H) represents intrinsic properties of the tissue (Fredberg and Stamenovic, 1989; Bates, 2009). In the PV curve, the static compliance (C_{ST}) measures the lung tissue distensibility; the estimate of inspiratory capacity (IC) is obtained from the volume of air received by the lungs up to a pressure of 30 cmH_2O; while the PV Loop Area indicates the amount of atelectasis (air-space closure) that existed before the PV-curve maneuver (West, 2012).

As mentioned above, data relating to respiratory mechanics are analyzed in terms of variations (Δ) of the variables, where Δ means the value for the parameter at time 30' minus its value at time 0'. Therefore, the results for respiratory system mechanics are presented in terms fraction of increase or decrease for each variable after 30 minutes of invasive ventilation, with an FiO_2 of either 21% associated with nebulized saline (Group 21%+S), or with 100% FiO_2 associated with either nebulized Eucalyptol (Group 100%+E) or saline (Group 100%+S). Regarding the results obtained during the FOT, a statistically significant increase was observed in the values of ΔR_N, ΔG and ΔH in the 100% + S group, when compared with the 21% + S group. The increase in ΔR_N may indicate increased stiffness of airway smooth muscle, which can be proven further in the analyses of lung parenchyma morphometry (Table 1, BCI) and histology (Figure 4, inserts). An increased R_N is expected when O_2 inhalation occurs in high concentrations due to changes in the airway epithelium, the arterial vascular bed, the alveolar septa, and the pleural spaces (Crapo, 1986).

Still, concerning ΔR_N, a statistically significant decrease was observed between the values for groups 100%+E and 100%+S, thus demonstrating attenuation of airway smooth muscle lesions when Eucalyptol is nebulized in association with an FiO_2 of 100%. This result is corroborated by the improvement seen in the photomicrographs (Figure 4, inserts) and a reduction in the values for BCI (Table 1, BCI).

The relaxing or bronchodilator effect of Eucalyptol on airway smooth muscle has been documented previously (Gondim et al., 2019; Kennedy-Feitosa et al., 2016). The use of Eucalyptol nebulization during high-FiO_2 IMV is a potential therapeutic strategy to attenuate the secondary damage caused by HALI and/or VILI in the smooth muscle of these patients' airways. Additionally, previous studies have observed that the lower airway is the primary target of infection in severe COVID-19 (Lee et al., 2020), thus making nebulized Eucalyptol during IMV an attractive option for reducing airway damage caused by SARS-CoV-2.

Resistance (G) and elastance (H) are related to the intrinsic properties of the pulmonary tissue; their values may be related to changes in tissue rheological properties (Bates, 2009). Regarding the results, a significant increase in the values of ΔG and ΔH for the animals in the 100%+S group compared with those of the 21%+S group. This indicates changes in the lung parenchyma caused by IMV with 100% FiO_2. The presence of alveolar septal thickening can confirm these changes, cell infiltrates (Figure 4), alveolar collapse (Figure 4 and Table 1), and the smaller mean alveolar diameter (L_m) (Table 1).

Hyperoxia causes the release of a large number of pro-inflammatory cytokines, such as interleukin 1-beta (IL-1ß) and tumor necrosis factor-alpha (TNF-α) (Ben-Ari et al., 2000); damage to type I pneumocytes (Lian et al., 2005); hyperplasia of type II pneumocytes (Babu et al., 2005); non-cardiogenic pulmonary edema (Song et al., 2000); alveolar hemorrhage with increased alveolar septum thickness (Dauger et al., 2003); and neutrophilic infiltration (Yamada et al., 2004). These findings corroborate the increased values for ΔG and ΔH of the animals in group 100% + S. A previous study analyzed oxidative damage and cellular infiltrates in lung parenchyma of animals exposed to an oxygen fraction of 100%, with significant tissue damage and macrophage infiltration being observed in animals exposed for even only 10 minutes (Valença et al., 2007).

There was also a statistically significant decrease in the values of ΔG and ΔH among the animals in the 100%+E group when compared with the 100%+S group. This indicates attenuation of damage at the level of the lung parenchymae of animals exposed to IMV with 100% FiO_2 associated with nebulized Eucalyptol. Previous studies have shown antioxidant and anti-inflammatory effects for Eucalyptol (Zhao et al., 2014; Kennedy-Feitosa et al., 2016), which may explain the improvement in these variables' values.

Previous studies have also shown increased serum levels of pro-inflammatory cytokines associated with pulmonary inflammation and extensive lung damage in SARS (Wong et al., 2004). Furthermore, lung injury caused by SARS-CoV-2 is characterized by pulmonary parenchyma destruction with interstitial inflammation (Nishiura et al., 2020). Thus, besides Eucalyptol displaying potential as a treatment option for the prevention of HALI and VILI, these results are yet another reason to

consider this oil as the possibility for the treatment of severe COVID-19 patients dependent on IMV with high FiO_2, as its capability to attenuate inflammation-associated increases in cell numbers and production of cytokines has been demonstrated. Thus, Eucalyptol may be a potentially significant agent in managing pulmonary inflammation (Kim et al., 2015).

Regarding the results obtained through the PV curves, a statistically significant change was observed in the values of ΔC_{ST}, ΔCI and $\Delta Area$, for the animals in the 100%+S group compared with the animals in the 100%+E group (Figure 2). The decreases in the ΔC_{ST} and ΔCI values may be associated, as a lower C_{ST} is related to increased lung tissue stiffness (Bates, 2009) or changes in alveolar surfactant (Wagers et al., 2001), thus creating more significant pressures for lung expansion, resulting in a lower CI. The increased $\Delta Area$ value for the animals in the 100%+S group can be attributed to various types of tissue changes, such as edema, alveolar collapse, and an increased presence of PMN cells (Table 1).

There was also a statistically significant change in the values of ΔC_{ST}, ΔCI and $\Delta Area$ for the animals in the 100% + E group compared with the animals in the 100% + S group (Figure 2). These findings support the previous discussion regarding the mitigation of secondary lung injury caused by IMV + 100% FiO_2, which is affected by the association of nebulized Eucalyptol with respiratory treatment.

Previous studies suggest that the production of surfactant proteins, along with other respiratory responses in the lungs of COVID-19 patients, could be downregulated (Islam et al., 2020); this reinforces the need for alternative treatments that improve C_{ST} in this disease, again rendering Eucalyptol nebulization an attractive option. Hysteresis was analyzed as an alternative method to assess lung injury caused by high-FiO2 IMV associated with Eucalyptol nebulization (the area between the inflating and deflating portions of the PV loop - Figure 3). The PV loop method has been shown to yield reliable results (Ingimarsson et al., 2003; Dyhr et al., 2004).

Plotting the PV curve is a technique used to obtain an objective diagnosis of the static mechanical properties of the respiratory system, having been adapted for use in intensive care unit (ICU) patients. Its application is usually reserved for patients with acute respiratory failure (ARF), including those with acute respiratory distress syndrome (ARDS), situations for which it has been proposed to observe the evolution of clinical severity. Regarding the results, Figure 3A shows the PV curves of animals in group S+21%. Data were obtained during the PV-curve maneuvers immediately after connecting the animal to the mechanical ventilator (21%+S-0') and 30 minutes after IMV with 21% FiO_2, performed with saline nebulization (21%+S-30'). An increased area and a shift in the curve to the right were observed at 21%+S-30', reflecting a decrease in C_{ST} And the presence of areas of atelectasis (West, 2012). These findings seem to reaffirm the induction of VILI by 30 minutes of IMV.

Figure 3B shows the PV curves of the animals in the 100%+S group. The data were obtained using PV-curve maneuvers immediately after connecting the subject to the ventilator (100%+S-0') and after 30 minutes of IMV + FiO_2 100% associated with saline aerosol (100%+S-30'). A sharp shift of the curve to the right and a marked increase in its area can be observed at 100%+S-30'. The strong shift to the right reflects the augmented C_{ST} (Bates, 2009), and the increased curve area indicates the need for greater pressure to open up areas of the lung due to atelectasis (Amato et al., 2015). These findings are in accordance with pulmonary parenchyma injury caused by HALI and VILI, the explanation for which was already reported above. Figure 3C shows the PV curves of animals of group E+100%; data collection occurred via PV-curve maneuvers performed immediately after the animal had been connected to the ventilator (100%+E-0') and again after 30 minutes' IMV using 100% FiO_2 and Eucalyptol nebulization (100%+E-30'). Although one can also observe at 100%+E-30' an increase in area and displacement of the curve to the right, curve layouts appear closer to those at 100%+E-0', compared with those of 100%+S-30'. This indicates an improvement in pulmonary parameters affected by the Eucalyptol treatment.

After analyzing all of the above results, we return to the initial hypothesis: Could the association of inhaled Eucalyptol to treatment with IMV + high FiO_2 be an appropriate strategy to minimize secondary lung injury caused by VILI and HALI in COVID-19 management? The answer is *yes*. Eucalyptol nebulization appears to be a promising candidate for use in IMV combined with oxygen therapy to prevent lung injury arising during the management of COVID-19. Furthermore, this therapy has the potential also to ameliorate the lung damage caused by SARS-CoV-2 infection itself since the angiotensin-converting enzyme (ACE) contributes significantly to the interaction of the SARS-CoV-2 with human cells (Zou et al., 2020), and Eucalyptol has already shown an ACE inhibitory effect (Dey et al., 2014).

This study has several limitations. First, due to technical restrictions, tests using groups of animals affected by SARS-CoV-2 were not carried out, which may limit the extrapolation of results. Secondly, it would be pertinent to perform analyses in groups exposed to lower FiO_2 values (e.g., 60%), which may more accurately portray the treatment of patients suffering from severe SARS coronavirus-2 infection (Angel et al., 2020). Thirdly, although the nebulized dose of 10 mg/mL has been reported previously (Kennedy-Feitosa et al., 2016), prior dose-response types of studies would have been able to find the lowest dose of Eucalyptol with the most significant effect.

CONCLUSION

In conclusion, evidence was found that treatment with nebulized Eucalyptol at a dose of 10 mg/mL effectively minimized pulmonary damage that would typically arise from HALI and VILI. This plant-derived oil is an attractive option in managing

patients presenting with severe forms of COVID-19 and who require IMV with high concentrations of oxygen. Thus, this study provides a starting point for further animal or clinical trials using this compound to treat lung lesions caused by managing infection caused by SARS-CoV-2 and the pulmonary damage caused by the virus itself.

CONFLICTS OF INTEREST

The authors declare that there is no conflict of interest regarding the publication of this manuscript.

ACKNOWLEDGEMENT

This study was financed in part by the Coordenação de Aperfeiçoamento de Pessoal de Nível Superior - Brasil (CAPES) - Finance Code 001.

REFERENCES

Amato, B., O. Meade and S. Slutsky, 2015. Driving pressure and survival in the acute respiratory distress syndrome. New England Journal of Medicine, 372(1):747–755. https://doi.org/10.1056/NEJMsa1410639

Angel, L., N. Kon and H. Chang, 2020. Novel percutaneous tracheostomy for critically ill patients with COVID-19. The Annals of thoracic surgery, 110(3):1006-1011. https://doi.org/10.1016/j.athoracsur.2020.04.010

Babu, R., A. Chidekel and H. Shaffer, 2005. Hyperoxia-induced changes in human airway epithelial cells: the protective effect of perflubron. Pediatric Critical Care Medicine, 6(2):188-194. https://doi.org/10.1097/01.PCC.0000154944.67042.4F

Barrasa, H., J. Rello and S. Tejada, 2020. SARS-CoV-2 in Spanish intensive care: early experience with 15-day survival in Vitoria. Anaesthesia Critical Care & Pain Medicine, 39(5):553-561. https://doi.org/10.1016/j.accpm.2020.04.001

Bates, J.T., 2009. Lung mechanics: An inverse modeling approach. Cambridge: Cambridge University Press.

Ben-Ari, J., R. Makhoul and J. Dorio, 2000. Cytokine response during hyperoxia: sequential production of pulmonary tumor necrosis factor and interleukin-6 in neonatal rats. The Israel Medical Association journal, 2(5):365-369.

Brower, G., A. Matthay and A. Morris, 2000. Ventilation with lower tidal volumes as compared with traditional tidal volumes for acute lung injury and the acute respiratory distress syndrome. New England Journal of Medicine, 342(18):1301-1308. https://doi.org/10.1056/NEJM200005043421801

Chen, N., M. Zhou and X. Dong, 2020. Epidemiological and clinical characteristics of 99 cases of 2019 novel coronavirus pneumonia in Wuhan, China: a descriptive study. The Lancet, 395(1023):507-513. https://doi.org/10.1016/S0140-6736(20)30211-7

Chorin, E., M. Dai and E. Shulman, 2020. The QT interval in patients with SARS-CoV-2 infection treated with hydroxychloroquine/azithromycin. MedRxiv, https://doi.org/10.1101/2020.04.02.20047050

Choy, T., L. Wong and P. Kaewpreedee, 2020. Remdesivir, lopinavir, emetine, and homoharringtonine inhibit SARS-CoV-2 replication in vitro. Antiviral research, 178:104786. https://doi.org/10.1016/j.antiviral.2020.104786

Crapo, J.D., 1986. Morphologic changes in pulmonary oxygen toxicity. Annual review of physiology, *48*(1), 721-731.

Dauger, S., L. Ferkdadji and G. Saumon, 2003. Neonatal exposure to 65% oxygen durably impairs lung architecture and breathing pattern in adult mice. Chest 123(2):530-538. https://doi.org/10.1378/chest.123.2.530

Dey, B., A. Mitra and P. Katakam, P, 2014. Exploration of natural enzyme inhibitors with hypoglycemic potentials amongst Eucalyptus Spp. by in vitro assays. World journal of diabetes 5(2):209. https://doi.org/10.4239/wjd.v5.i2.209

Duan, K., B. Liu and C. Li, 2020. Effectiveness of convalescent plasma therapy in severe COVID-19 patients. Proceedings of the National Academy of Sciences, 117(17):9490-9496. https://doi.org/10.1073/pnas.2004168117

Dyhr, T., E. Nyga˚rd and N. Laursen, 2004. Both a lung recruitment maneuver and PEEP are needed to increase oxygenation and lung volume after cardiac surgery. Acta Anaesthesiologica Scandinavica, 48(1):187–97. https://doi.org/10.1111/j.0001-5172.2004.00300.x

Forrester, J., W. Booz and D. Sigmund, 2018. Angiotensin II signal transduction: an update on mechanisms of physiology and pathophysiology. Physiological reviews, 98(3):1627-1738. https://doi.org/10.1152/physrev.00038.2017

Fredberg, J., Stamenovic, D., 1989. On the imperfect elasticity of lung tissue. Journal of applied physiology, 67(6), 2408–2419.

Gondim, L., D. Serra and A. Cavalcante, 2019. Effects of Eucalyptol in respiratory system mechanics on acute lung injury after exposure to short-term cigarette smoke. Respiratory physiology & neurobiology, 266(1):33-38. https://doi.org/10.1016/j.resp.2019.04.007

Hantos, Z., B. Daroczy and B. Suki, 1992. Input impedance and peripheral inhomogeneity of dog lungs, Journal of applied physiology, 72(1):168–178. https://doi.org/10.1152/jappl.1992.72.1.168

ICNARC. 2016. Key statistics from the Case Mix Programme — adult, general critical care units. https://www.icnarc.org/Our-Audit/Audits/Cmp/Reports/Summary-Statistics. Accessed 10 June 2020

Ingimarsson, J., J. Bjo¨rklund and T. Curstedt, 2003. A lung recruitment maneuver immediately before rescue surfactant therapy does not affect the lung mechanical response in immature lambs with respiratory distress syndrome. Acta anaesthesiologica scandinavica, 47(8):968–72. https://doi.org/10.1034/j.1399-6576.2003.00202.x

Islam, B., and K. Khan, 2020. Lung biopsy cells transcriptional landscape from COVID-19 patient stratified lung injury in SARS-CoV-2 infection through impaired pulmonary surfactant metabolism. bioRxiv. https://doi.org/10.1101/2020.05.07.082297

Ismael-Badarneh, R., J. Guetta and G. Klorin, 2015. The role of angiotensin II and cyclic AMP in alveolar active sodium transport. PloS one, 10(8):e0137118. https://doi.org/10.1371/journal.pone.0137118

Kapitan, S., 2013. Ventilatory failure. Can you sustain what you need? Ann Am Thorac Soc 10:396–399. https://doi.org/10.1513/AnnalsATS.201305-132OT

Kennedy-Feitosa, E., T. Okuro and V. Pinho, 2016. Eucalyptol attenuates cigarette smoke-induced acute lung inflammation and oxidative stress in the mouse. Pulmonary Pharmacology & Therapeutics, 41(1):11-18. https://doi.org/10.1016/j.pupt.2016.09.004

Kim, Y., S. Lee and H. Seol, 2015. Eucalyptol suppresses matrix metalloproteinase-9 expression through an extracellular signal-regulated kinase-dependent nuclear factor-kappa B pathway to exert anti-inflammatory effects in an acute lung inflammation model. Journal of Pharmacy and Pharmacology, 67(8):1066-1074. https://doi.org/10.1111/JPHP.12407

Knudsen, L., R. Weibel and G. Gundersen, 2009. Assessment of air space size characteristics by intercept (chord) measurement: an accurate and efficient stereological approach. Journal of applied physiology, 108 (2):412-421. https://doi.org/10.1152/japplphysiol.01100.2009

Lee, I., L. Hu and Y. Chen, 2020. Are children less susceptible to COVID-19?. Journal of Microbiology, Immunology, and Infection. 53(3):371–372. https://doi.org/10.1016/j.jmii.2020.02.011

Li, F., K. Liao and S. Ko, 2007. Hyperoxia increases ventilator-induced lung injury via mitogen-activated protein kinases: a prospective, controlled animal experiment. Critical care 11(1), R25.

Li, T., H. Lu and W. Zhang, 2020. Clinical observation and management of COVID-19 patients. Emerging Microbes & Infections, 9(1):687-690, https://doi.org/10.1080/22221751.2020.1741327

Li, Y., Y. Lai and Y. Wang, 2016. 1, 8-Cineol protect against influenza-virus-induced pneumonia in mice. Inflammation. 39(4):1582-1593. https://doi.org/10.1007/s10753-016-0394-3

Lian, X., Y. Qin and A. Hossain, 2005. Overexpression of Stat3C in pulmonary epithelium protects against hyperoxic lung injury. The Journal of Immunology, 174(11):7250-7256.

Liu, J., R. Cao and M. Xu, 2020. Hydroxychloroquine, a less toxic derivative of chloroquine, is effective in inhibiting SARS-CoV-2 infection in vitro. Cell discovery, 6(1):1-4. https://doi.org/10.1038/s41421-020-0156-0

Murthy, S., D. Gomersall and A. Fowler, 2020. Care for critically ill patients with COVID-19. JAMA. 2020;323(15):1499-1500. https://doi.org/10.1001/jama.2020.3633

Ñamendys-Silva SA (2020) Respiratory support for patients with COVID-19 infection. The Lancet Respiratory Medicine, 8(4), e18. https://doi.org/10.1016/S2213-2600(20)30110-7

Nascimento, R., C. Refosco and F. Vasconcelos, 2009. 1,8-Cineole induces relaxation in rat and guinea-pig airway smooth muscle. The Journal of Pharmacy and Pharmacology, 61(3), 361–366. https://doi.org/10.1211/jpp.61.03.0011

Nieman, F., J. Satalin and P. Andrews, 2017. Personalizing mechanical ventilation according to physiologic parameters to stabilize alveoli and minimize ventilator induced lung injury (VILI). Intensive care medicine experimental, 5(1):1-21. https://doi.org/10.1186/s40635-017-0121-x

Nishiura, H., M. Jung and M. Linton, 2020. The extent of transmission of novel coronavirus in Wuhan, China. Journal of clinical medicine, 9(2):330. https:/doi.org/10.3390/ jcm9020330

Reid, D., J. Huang and S. Bryson, 1994. Diaphragm injury and myofibrillar structure induced by resistive loading. Journal of applied physiology, 76(1):176-184.

Rello, J., E. Storti and M. Belliato, 2020. Clinical phenotypes of SARS-CoV-2: Implications for clinicians and researchers. European Respiratory Journal, *55*(5). https://doi.org/10.1183/13993003.01028-2020

Richardson, S., S. Hirsch and M. Narasimhan, 2020. Presenting characteristics, comorbidities, and outcomes among 5700 patients hospitalized with COVID-19 in the New York City area. JAMA. 323(20):2052-2059. https://doi.org/10.1001/jama.2020.6775

Sakae, S., S. Leme and M. Dolhnikoff, 1994. Neonatal capsaicin treatment decreases airway and pulmonary tissue responsiveness to methacholine. American Journal of Physiology-Lung Cellular and Molecular Physiology. 266 (1):23-29. https://doi.org/10.1152/ajplung.1994.266.1.L23

Shen, C., Z. Wang, and F. Zhao, 2020. Treatment of 5 critically ill patients with COVID-19 with convalescent plasma. JAMA, 323(16):1582-1589. https://doi.org/10.1001/jama.2020.4783

Singh, K., A. Singh and A. Shaikh, 2020. Chloroquine and hydroxychloroquine in the treatment of COVID-19 with or without diabetes: A systematic search and a narrative review with a special reference to India and other developing countries. Diabetes & Metabolic Syndrome: Clinical Research & Reviews. https://doi.org/10.1016/j.dsx.2020.03.011

Song, Y., N. Fukuda and C. Bai, 2000. Role of aquaporins in alveolar fluid clearance in neonatal and adult lung, and in oedema formation following acute lung injury: studies in transgenic aquaporin null mice. The Journal of physiology 525(3):771-779.

Sriram, K., and A. Insel, 2020. A hypothesis for pathobiology and treatment of COVID-19: The centrality of ACE1/ACE2 imbalance. British Journal of Pharmacology. Juergens UR, Engelen T, Racké K, Stöber M, Gillissen A, Vetter H. Inhibitory activity of 1, 8- cineol (Eucalyptol) on cytokine production in cultured human lymphocytes and monocytes. Pulmonary pharmacology & therapeutics ,17(5):281-287. https://doi.org/10.1016/J.PUPT.2004.06.002

Sun, Q., H. Qiu and M. Huang, 2020. Lower mortality of COVID-19 by early recognition and intervention: experience from Jiangsu Province. Annals of Intensive Care, 10(1):33. https://doi.org/10.1186/s13613-020-00650-2

Valença, S., L. Kloss and S. Bezerra, 2007. Effects of hyperoxia on Wistar rat lungs. Brazilian Journal of Pulmonology, 33(6):655-662. https://doi.org/10.1590/S1806-37132007000600008

Wagers, S., K. Lundblad and M. Ekman, 2004. The allergic mouse model of asthma: normal smooth muscle in an abnormal lung. Journal of Applied Physiology, 96(1):2019-2027.

Wang, D., B. Hu and C. Hu, 2020. Clinical characteristics of 138 hospitalized patients with 2019 novel coronavirus–infected pneumonia in Wuhan, China. JAMA, 323(11):1061-1069. https://doi.org/10.1001/jama.2020.1585

Wang, Y., D. Zhang and G. Du, 2020. Remdesivir in adults with severe COVID-19: a randomized, double-blind, placebo-controlled, multicentre trial. The Lancet, 395(10236):1569-1578. https://doi.org/10.1016/S0140-6736(20)31022-9

Weibel, E.R., 1990. Morphometry: stereological theory and practical methods. In: Models of Lung Disease: Microscopy and Structural Methods, edited by Gil J. New York: Marcel Dekker. 199–247.

West, J.B., 2012. Respiratory physiology; The essentials, 9th edition; Chapter 7, the mechanics of breathing.

WHO - World Health Organization. Clinical management of Severe Acute Respiratory infection (SARI) when COVID-19 disease is suspected. 2020.

Wong, K., W. Lam and K. Wu, 2004. Plasma inflammatory cytokines and chemokines in severe acute respiratory syndrome. Clinical & Experimental Immunology, 136(1):95-103. https://doi.org/10.1111/j.1365-2249.2004.02415.x

Yamada, M., H. Kubo and S. Kobayashi, 2004. Interferon-γ: a key contributor to hyperoxia-induced lung injury in mice. American Journal of Physiology-Lung Cellular and Molecular Physiology, 287(5):L1042-L1047. https://doi.org/10.1152/ajplung.00155.2004

Yao, X., F. Ye and M. Zhang, 2020. In vitro antiviral activity and projection of optimized dosing design of hydroxychloroquine for the treatment of severe acute respiratory syndrome coronavirus 2 (SARS-CoV-2). Clinical Infectious Diseases, 71(15):732-739. https://doi.org/10.1093/cid/ciaa237

Zhang, B., S. Liu and T. Tan, 2020. Treatment with convalescent plasma for critically ill patients with SARS-CoV-2 infection. Chest, 158(1), e9-e13. https://doi.org/10.1016/j.chest.2020.03.039

Zhao, C., J. Sun and C. Fang, 2014. 1, 8-cineol attenuates LPS-induced acute pulmonary inflammation in mice**.** Inflammation 2(37):566-572. https://doi.org/10.1007/s10753-013-9770-4

Zhou, F., T. Yu and R. Du, 2020. Clinical course and risk factors for mortality of adult inpatients with COVID-19 in Wuhan, China: a retrospective cohort study. Lancet, 395(1):1054-1062. https://doi.org/10.1016/S0140-6736(20)30566-3

Zhou, Y., F. Wang and D. Tang, 2007. Inhibitory effect of 1, 8-cineol (eucalyptol) on Egr-1 expression in lipopolysaccharide-stimulated THP-1 cells 1. Acta pharmacologica sinica, 6:908-912. https://doi.org/10.1111/j.1745-7254.2007.00555.x

Zou, X., K. Chen and J. Zou, 2020. Single-cell RNA-seq data analysis on the receptor ACE2 expression reveals the potential risk of different human organs vulnerable to 2019-nCoV infection. Frontiers of Medicine, 14(2):185–192 https://doi.org/10.1007/s11684-020-0754-0